The Franck-Hertz Experiment

Andy Chmilenko, Nick Kuzmin
Instructor: Jeff Gardiner, David Hawthorn
Section 1
(Dated: 1:30 pm Monday June 9, 2014)

I. ABSTRACT

This experiment undertakes an experimental analysis of the Franck-Hertz method for finding the energy gaps and ground state of mercury. It accounts for the effect of the acceleration of electrons over their mean-free-paths on the energy gap distribution and size, and provides a comparison to the results obtained by Rapior, Sengstock, and Baev in their paper on the new characteristics of the Franck-Hertz experiment (from which the analysis included in this paper is taken). Data is taken for a range of temperatures between 150 °C and 200 °C, from which a value of E_a=4.70 ±0.88 eV is calculated for the ground state of mercury. Calculations of the mean-free-path of electrons at each temperature, but no trend is found mainly due to the limitations of the Franck-Hertz apparatus used in the experiment.

II. INTRODUCTION

The quantum description of particles has increasing become important in modern physics, but it not quite so obvious or intuitive. It is known that photons are contained in quantized packets of energy equal to $\Delta E = h\nu$ through the photoelectric effect, at the time the same wasn't known about atoms and their bound electrons. The atom is relatively unknown in its make-up, although Bohr's model was good at answering many of the new observed phenomena in encountered in physics. Just as it was observed that certain atoms can only emit photons at specific wavelengths, the Franck-Hertz experiment confirmed that they also absorb energies related to the energy levels of bound electron states as theorized by the Bohr model of the atom, helping pave the way to better understanding not only Quantum Mechanics, but the behaviour of atoms.

Using a placing a vacuum tube filled with mercury vapour inside an oven, that has a filament producing electrons which are accelerated through the mercury (Hg) gas using an anode and cathode grid, the current of electrons can be collected. By varying the temperature of the tube system using the oven, the concentration of Hg gas can be controlled, and thus the interaction between accelerated electrons and Hg atoms can be studied. By measuring the received current as a function of the accelerating potential and varying the temperature of the tube to have an optimal concentration of Hg atoms, the electrons can undergo inelastic collisions with the Hg atoms and lose some energy equal to the energy between excitation levels of Hg, which experimentally, the lowest is known to be 4.67 electron volts (eV) ($6^1S_0 \rightarrow 6^3P_0$), or the second last excited state 4.89 eV ($6^1S_0 \rightarrow 6^3P_1$), or to the third last excited state of 5.46 eV ($6^1S_0 \rightarrow 6^3P_2$).

III. THEORETICAL BACKGROUND

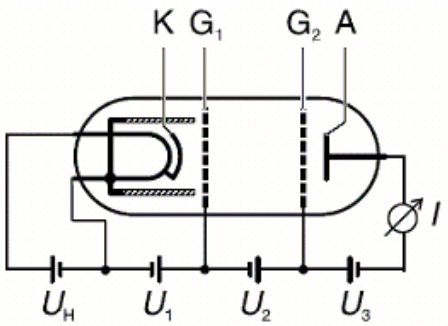

FIG. 1: Schematic diagram of the Franck-Hertz Tube, where K is the Cathode filament, G_1 and G_2 are the accelerating grids, and A is the Anode.

The Franck-Hertz Tube, shown schematically in Fig.1, is typically a sealed tube filled with, in this case Mercury and contained an Cathode filament which produces free electrons which are then accelerated initially by grid G_1 controlled by voltage U_1. The Franck-Hertz control unit varies voltage U_2 applied between grid G_1 and G_2, so that electrons accelerated through this region can have enough energy to inelastically collide with Hg atoms. A small retarding voltage, U_3 is applied between grid G_2 and the anode A so that electrons that collide inelastically with Hg atoms in that region, don't have enough energy to overcome that potential barrier and make it to the anode. The resulting current in the anode A is up-amped and measured. In each trial, U_1 and U_3 are held constant while U_2 is varied between 0 to 30 V automatically by the Franck-Hertz control unit.

The Franck-Hertz tube is housed in an oven with an attached thermocouple so that the temperature of the tube can be controlled accurately. By controlling the temperature of the tube the concentration of the Hg atoms as a vapour can be controlled. Controlling the concentration of Hg atoms is important because that affects the mean free path (MFP) of the electron given by:

$$MFP = \lambda = \frac{1}{N\sigma} \tag{1}$$

where N is the number density of Hg atoms, and σ is the cross-sectional area of the Hg atoms. The cross-sectional area is given by,

$$\sigma = \pi(r_1 + r_2)^2 \tag{2}$$

then using the ideal gas law,

$$\rho V = nk_bT \tag{3}$$

where the number density $N = \frac{n}{V}$, the MFP becomes:

$$MFP = \lambda = \frac{k_BT}{\rho\sigma} = \frac{k_BT}{\rho\pi r^2} \tag{4}$$

where k_B is Boltzmann's constant, T is the temperature in Kelvin, ρ is the pressure in Pa, and r is the radius of the Hg atom, the radius of the electron is assumed to be $r_e \ll r_{Hg}$.

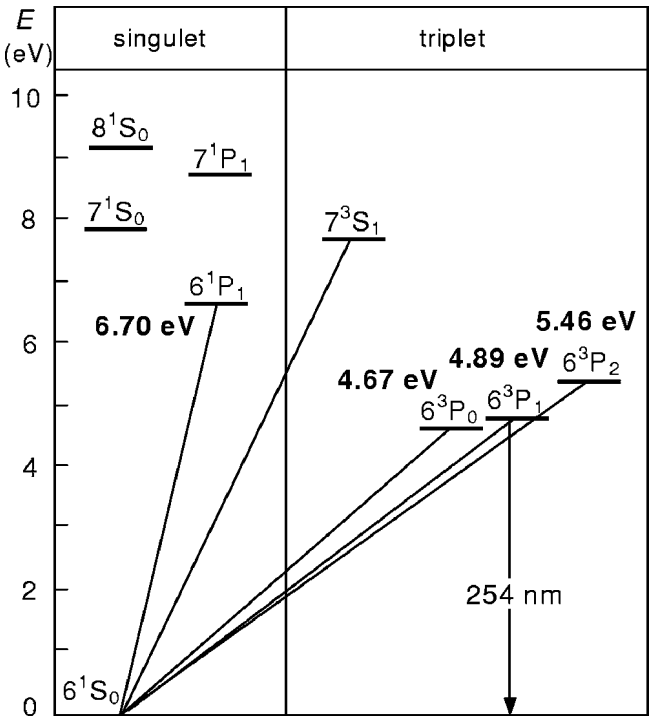

FIG. 2: Last energy levels in Hg (Ref. 6).

When the MFP is significantly smaller than the distance L, from G_1 to G_2, such that the electrons will collide with the Hg atoms inside the tube and lose some energy. The electrons will only lose energy equal to the discrete energy states of the Hg atoms from collision excitation, in this case is most commonly excited states between 4.67 eV and 5.47 eV as seen in Fig.2. As U_2 is varied and the electrons are accelerated between G_1 and G_2, when the electron doesn't have enough energy to excite the Hg atom, the anode A will see an increase in current. However as U_2 increases and accelerates electrons to a point where they have enough energy to excite the Hg atoms, the electrons will lose all or most their kinetic energy, then due to the retarding voltage U_3, the low energy electrons will not be able to make it to the anode A and will fall back onto G_2, so there will be a 'dip' in the measured current. As U_2 increases more, electrons that excite an Hg atom and are accelerated to a point where they have enough energy for a second excitation though inelastic collision, there will be another dip in the measured current at A. The same goes for electrons that can have three or more inelastic collisions between G_1 and G_2 as U_2 increases between 0 and 30 V.

The MFP can also be determined from the spacing between minima by following the reasoning at, as an electron is accelerated though the tube and reaches a point where it just has enough energy to excite an Hg atom in an inelastic collision, the electron will gain some small energy δ_1 on average before it collides with an Hg atom, travelling a distance equal to the MFP, λ having an enegy $E = E_a + \delta_1$. For two inelastic collisions at the same number density of Hg atoms, the electron will have a greater additional energy $\delta_2 > \delta_1$ since the accelerating potential is greater, thus the electron will have gained energy $E = 2E_a + 2\delta_2$. For n collisions we can then express the gained energy as:

$$E_n = n(E_a + \delta_n) \tag{5}$$

where δ_n is the n^{th} order minima and is a function of the distance L between G_1 and G_2, the MFP (λ), and the minimum excitation energy E_a:

$$\delta_n = n\frac{\lambda}{L}E_a \tag{6}$$

From this, using Eq.5 and Eq.6 and rearranging, we can get an expression for the change in energy between minima on the measured Franck-Hertz curve.

$$\begin{gathered}
\Delta E(n) = E_n - E_{n-1} \\
\Delta E(n) = n(E_a + \delta_n) - (n-1)(E_a + \delta_{n-1}) \\
\Delta E(n) = n(E_a + n\tfrac{\lambda}{L}E_a) - (n-1)(E_a + (n-1)\tfrac{\lambda}{L}E_a) \\
\Delta E(n) = E_a[n(1 + n\tfrac{\lambda}{L}) - (n-1)(1 + n\tfrac{\lambda}{L} - \tfrac{\lambda}{L})] \\
\Delta E(n) = E_a[\cancel{n} + n^2\tfrac{\lambda}{L} - \cancel{n} - n^2\tfrac{\lambda}{L} + n\tfrac{\lambda}{L} + 1 + n\tfrac{\lambda}{L} - \tfrac{\lambda}{L}] \\
\Delta E(n) = E_a[2n\tfrac{\lambda}{L} + 1 - \tfrac{\lambda}{L}]
\end{gathered}$$

$$\Delta E(n) = E_a[1 + \frac{\lambda}{L}(2n-1)] \tag{7}$$

Equation 7 can than be rearranged for an alternate expression for the MFP as follows:

$$\lambda = \frac{L}{2E_a}\frac{d\Delta E(n)}{dn} \tag{8}$$

IV. EXPERIMENTAL DESIGN AND PROCEDURE

Apparatus:

- Control Unit for Franck-Hertz Tube
- Franck-Hertz Tube
- Oven for Franck-Hertz Tube
- Temperature probe, NiCr-Ni
- Digital Voltmeter
- USB data acquisition card for Labview and wires
- Computer with LabView and acquisition program

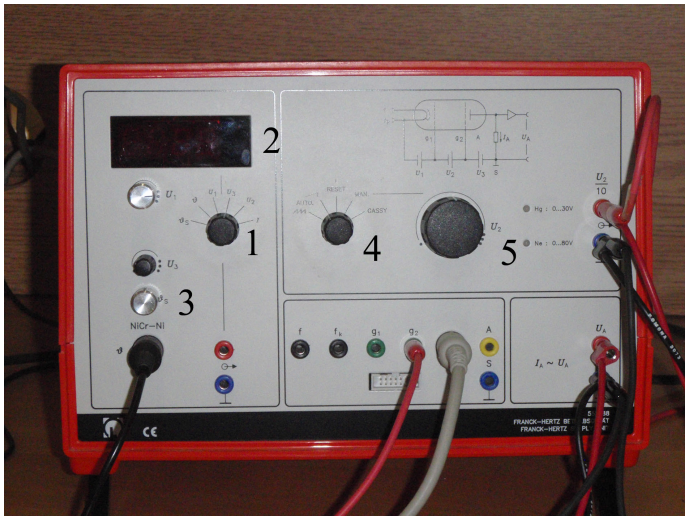

FIG. 3: The Franck-Hertz control unit with labelled points of interest

Once the equipment was turned on, the target temperature on the Control Unit for the Franck-Hertz Tube needed to be set to around 140°C using the ϑ_S knob, the attached oven unit needed time to heat up to the desired temperature before attempting the rest of the experiment. After verifying the Franck-Hertz Tube has reached the target temperature (as measured by the thermocouple) by setting knob 1 (as seen in Fig.3) to ϑ and reading the temperature off of the built-in LED screen, the data acquisition begin.

Having the LabView software open on the attached computer with the Franck-Hertz data acquisition program running, by first having knob 4 on the Franck-Hertz control unit set to 'RESET' then pressing the play button and simultaneously switching knob 4 from 'RESET' to the Ramp setting, the data acquisition began. If the acquired data didn't have 5 visible peaks, the knobs U_1 and U_3 were adjusted and the program was stopped to clear the data and new data was reacquired using the same steps. Once an adequate graph was acquired and it had about 5 visible peaks, the data was saved to the computer by pressing the button labelled 'STOP' in the program.

Data for the anode voltage versus acceleration potential was acquired for five different temperatures more or less evenly spaced out between 140-200°C in the same fashion as above, making sure to wait for the Franck-Hertz Tube to reach the target temperature (as measured by the thermocouple unit) and adjusting knobs U_1 and U_3 before continuing with the data acquisition.

Afterwards, the Franck-Hertz Tube was left to cool down to a temperature such that when data from the Franck-Hertz control unit was acquired in the fashion above, no peaks could be observed, but only an increasing function could be observed and the data was saved as a baseline when electrons do not interact with anything inside the tube.

Before leaving the lab, the distance between the anode and the cathode of the Franck-Hertz Tube was measured roughly and recorded.

V. ANALYSIS

Before data was taken in the experiment, the effects of varying voltages U_1 and U_3 were noted. As the latter facilitates the thermionic emission of electrons from the cathode, decreasing it decreased the total amount of free electrons, and thereby the current detected at the anode. Decreasing U_3 on the other hand, increased the current due to the lower voltage necessary for electrons to overcome before reaching the anode. It was important to adjust and balance these voltages for each temperature, as having too low a value of U_3 would introduce too much noise, while too high a value of would cut off too much of the current too obtain an accurate Franck-Hertz characteristic. Similarly, the wrong value of U_1 could either quench the amount of free electrons available, or create too large of a contribution compared to the main accelerating voltage, U_2.

The Child-Langmuir Law characterizes the maximum current within the anode that results from the electric potential that exists between the anode and cathode. This current is limited by the space charge in the vacuum tube. It states that for a fixed anode-cathode separation, the anode current is a function of the three-halves power of the anode voltage.

$$I_A = \frac{4\epsilon_0 S V_A^{\frac{3}{2}}}{9d^2}\sqrt{\frac{2e}{m_e}} \tag{9}$$

Where S is the surface area of the anode (given in this case by $2\pi rh$) d is the distance between the two grids (G_1 and G_2), and $\frac{e}{m_e}$ is the electron's charge to mass ratio.

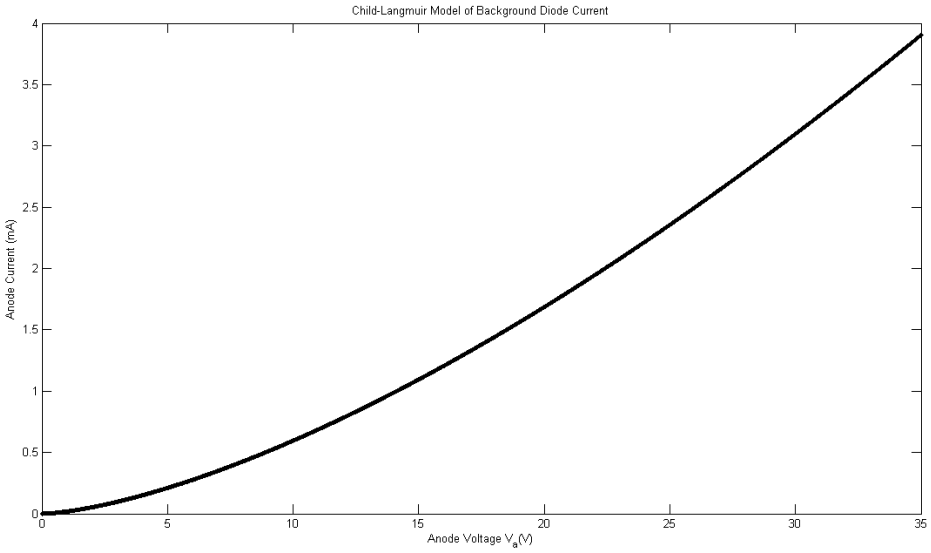

FIG. 4: Background anode current versus accelerating potential U_2 showing the Child-Langmuir Law

Figure 4 gives the Child's Law correction for values of $d = 7$ mm, $r = 9$ mm, and $h = 7$ mm. While the correction appears small, it is enough to shift troughs in the Franck-Hertz characteristics by several hundredth of millivolts. As the background is not constant (or linear, for that matter), it cannot be assumed that the locations of the minima will remain the same once the background current has been subtracted, making the Child's Law correction necessary for accurate results.

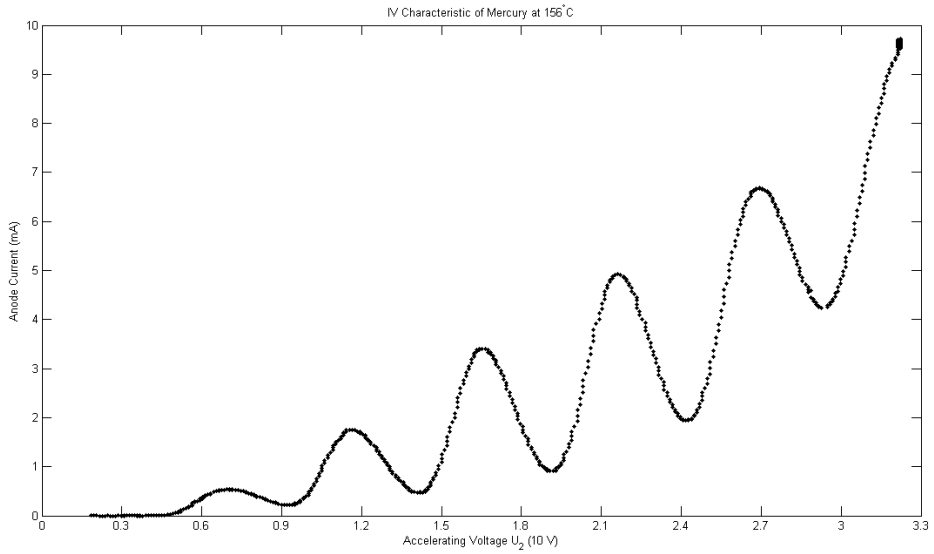

FIG. 5: Anode current versus accelerating potential U_2 with the Franck-Hertz tube at 156°C

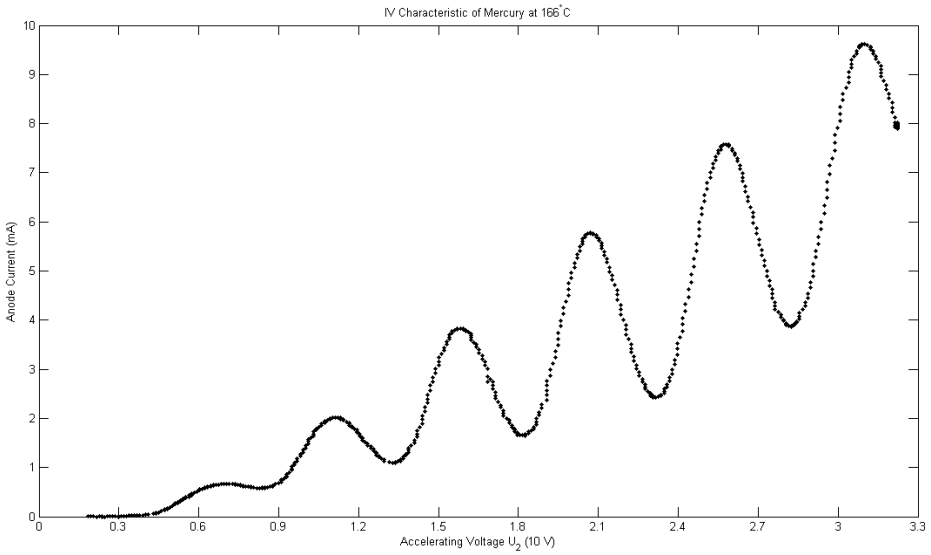

FIG. 6: Anode current versus accelerating potential U_2 with the Franck-Hertz tube at 166°C

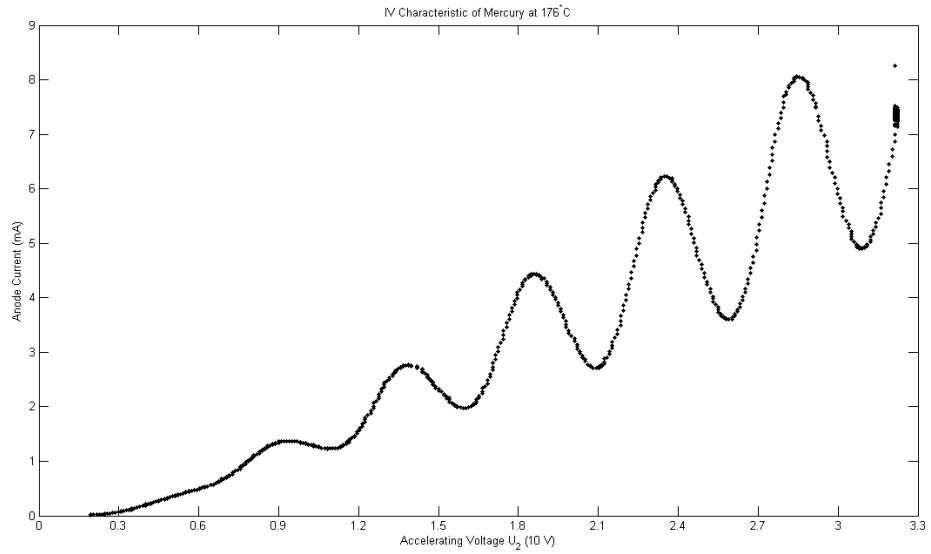

FIG. 7: Anode current versus accelerating potential U_2 with the Franck-Hertz tube at 176°C

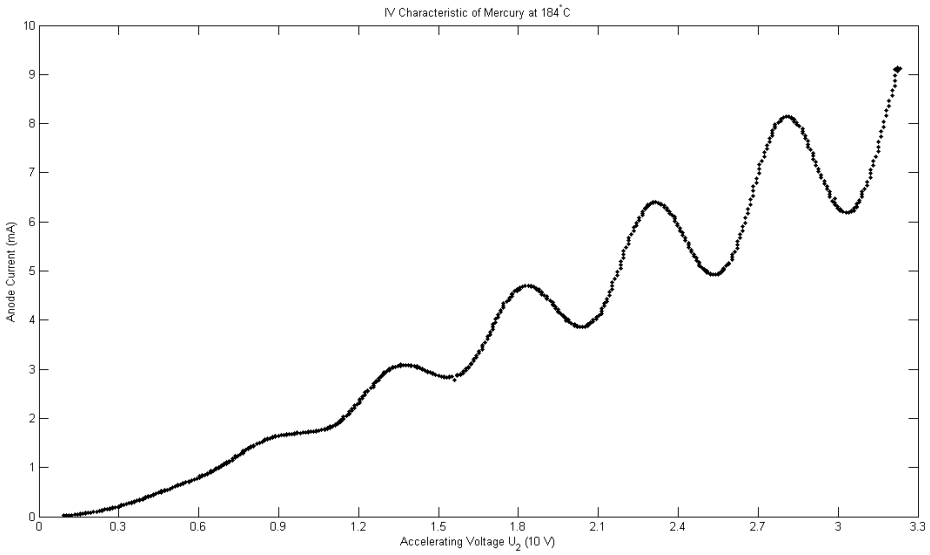

FIG. 8: Anode current versus accelerating potential U_2 with the Franck-Hertz tube at 184°C

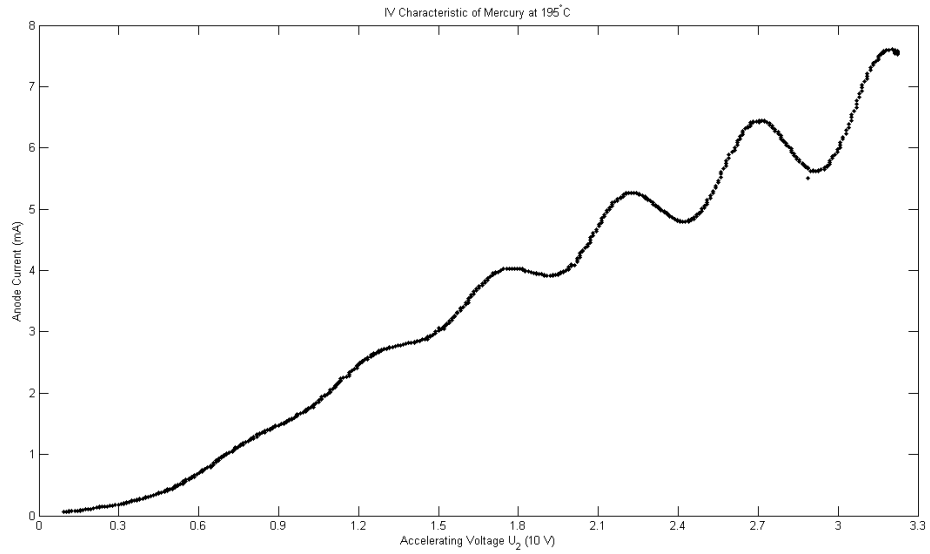

FIG. 9: Anode current versus accelerating potential U_2 with the Franck-Hertz tube at 195°C

Figures 6 through 9 present the Franck-Hertz characteristics of gaseous Hg that were obtained at different temperatures. It should be noted that as the temperature was increased, it became increasingly difficult to obtain reliable locations for the minima so some of the higher temperature results were discarded. On top of this, the Matlab code used to identify the minima ran into difficulties as there was a great deal of variation in the current around each minima, making it difficult to select from the variety of voltages at which they occurred. This was most likely caused by the limitations of the Franck-Hertz apparatus used in the laboratory.

E_A(eV)					
156 °C	**166 °C**	**176 °C**	**184 °C**	**195 °C**	**Average**
4.764	4.699	4.862	4.535	4.627	4.697
± 2.307	± 1.071	± 2.688	± 2.262	± 0.600	± 0.876

TABLE I: Tabulated results for measured excitation level of Hg for the different tube temperatures.

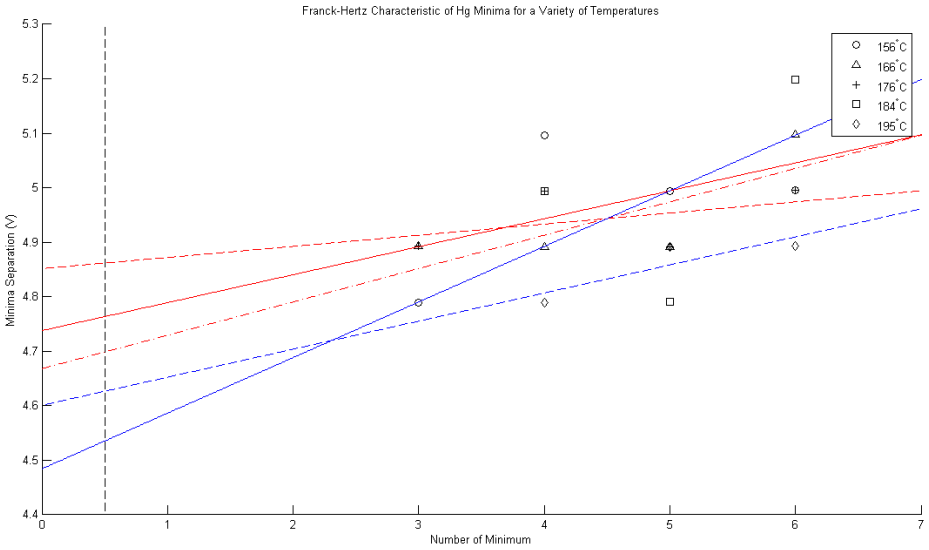

FIG. 10: Minima separation plotted against the minima number, for the 5 trials of the Franck-Hertz experiment

Figure 10 presents the compiled results of the five Franck-Hertz characteristics. Linear regression was used to model each set of data, with the error in slope taken from the respective coefficients of determination (R squared). These values were used to extrapolate the ground state energies and their associated error, which were then averaged to give the final value of E_A. The results are presented in Table I.

The experimentally obtained value of 4.697eV differs from the value of 4.65 eV obtained in the Rapior paper by only 1.01%. While the former is outside of the error of 0.03 eV in Rapior's result, the substantially larger error of 0.876 eV obtained in this experiment. The cause of such a large error comes from the error in the linear regression model used to model the data, which in turn was caused by the aforementioned imprecision in the Franck-Hertz apparatus. It is also possible that it was the result of a flawed Child's Law approximation of the anode current, as the anode's surface area was difficult to judge. Furthermore, grids G_1 and G_2, and their proximity to other components could have introduced other interactions, such as residual capacitances, that would have modified the relation describing the current background.

Mean-Free-Path, λ (μm)				
156 °C	**166 °C**	**176 °C**	**184 °C**	**195 °C**
37.69	45.59	14.69	78.72	38.96
±18.45	±10.89	±0.819	±39.66	± 0.577

TABLE II: Tabulated results for measured Mean-Free-Path, λ, of electrons for the different tube temperatures.

Table II details the values of the electron mean-free-path for each temperature. It is immediately clear that there is no unifying pattern or trend among the data, and the uncertainties are accordingly large. As the error does not appear to come from a consistent source propagating across the data, it is more likely that the limited precision of the Franck-Hertz apparatus is once again responsible. As the error margins are calculated from the errors on the respective energy gap and the R-squared values of the linear regression models, the non-linear distribution of data points easily upsets any relationship between the temperature and energy gaps. It is interesting that despite the

significant error in slopes, the value of the ground state of mercury was still extremely close to the predicted value. It is possible the approximation that $\lambda \ll L$ was at least partially involved, as the theoretically predicted values modelled by Eq. 4 are only one order below the grid separation at the lower temperatures. While smaller, they might still be large enough that the approximation ceases to hold.

The theoretically predicted values themselves were obtained under the assumption the cross sectional radius of the mercury atom was the atomic radius of 151 pm. While this does not produce the same cross sectional area as that used by Rapior, the difference is made up by the differing models for the vapour pressure of mercury used between this experiment and Rapior's analysis (approximately linear between the known values listed in Malestrom's handbook of physics and chemistry, as opposed to the exponential model used by Rapior).

VI. CONCLUSION

The analysis of the data obtained in this experiment yielded a value of 4.70 ±0.88 eV for the ground state of mercury, E_A. This result differs by 1.01% from that obtained by Rapior, Sengstock, and Baev in their paper on the new features of the Franck-Hertz experiment. The mean free paths of electrons at 155 °C, 165 °C, 175 °C, 184 °C, and 195 °C were determined to be 37.69 ±18.45 μm, 45.59 ±10.89 μm, 14.69 ±0.819 μm, 78.72 ±39.66 μm, and 38.96 ±0.577 μm respectively. The mean free paths did not show the predicted trend of decreasing with temperature, and exhibited high error. This error is expected to be caused by the limitations of the Franck-Hertz apparatus used in this experiment, and of effects on the anode current other than those predicted by the Child-Langmuir model.

VII. REFERENCES

1. Jeff Gardiner. The Franck-Hertz Experiment. Waterloo, Ontario: University of Waterloo; c2014. 3 p.

2. Adrian C. Melissios. Experiments in Modern Physics. Second Edition. New York and London: Academic Press, 1966. 288p.

3. Rapior G, Sengstock K, Baeva V. 2006. New features of the Franck-Hertz experiment. Am. J. Phys. 74(5):423-428. 10.1119/1.2174033.

4. Robert Eisberg, Robert Resnick. Quantum Physics of Atoms, Molecules, Solids, Nuclei, and Particles. Second Edition. New York: John Wiley & Sons, 1985. 866p.

5. LD Didactic Group. [Internet]. Germany: LD DIDACTIC GmbH. [cited 2014 June 23]. Available from: `http://www.ld-didactic.de/documents/en-US/EXP/P/P6/P6241_e.pdf`

6. H. Haken and H. C. Wolf. The Physics of Atoms and Quanta. 6th ed. Springer, Heidelberg, 2000. 305p.

7. David R. Lide, Willam M. Haynes. CRC Handbook of Chemistry and Physics. Sixth Edition. Boca Raton (Fla.), CRC Press, 2009. 2692p.